PERGAMON

International Journal of Solids and Structures 39 (2002) 4291–4310

INTERNATIONAL JOURNAL OF SOLIDS and STRUCTURES

www.elsevier.com/locate/ijsolstr

On static analysis of finite repetitive structures by discrete Fourier transform

E.G. Karpov [a,*], N.G. Stephen [a], D.L. Dorofeev [b]

[a] *Mechanical Engineering, School of Engineering Sciences, University of Southampton, Highfield, Southampton SO17 1BJ, United Kingdom*

[b] *Department of Mathematical Physics, Voronezh State University, Universitetskaya Sq. 1, Voronezh 394693, Russian Federation*

Received 16 May 2001; received in revised form 21 March 2002

Abstract

Functional solutions for the static response of beam- and plate-like repetitive lattice structures are obtained by discrete Fourier transform. The governing equation is set up as a single operator form with the physical stiffness operator acting as a convolution sum and containing a matrix kernel, which relates to the mechanical properties of the lattice. Boundary conditions do not affect the equation form, and are taken into account at a subsequent stage of the analysis. The technique of virtual load and substructure is proposed to formally close the repetitive lattice into a cyclic structure, and to assure the equivalence of responses of the modified cyclic and original repetitive lattices. A discrete periodic Green's function is introduced for the modified structure, and the final displacement solutions are written as convolution sums over the Green's function and the actual external and virtual loads. Several example problems illustrate the approach.

Keywords: Repetitive structures; Static response; Discrete Fourier transform; Green's function

1. Introduction

A structure is said to be repetitive when its construction takes the form of a spatially regular lattice or pattern of elements. A regular bridge framework, and honeycomb panel are examples of 1-D (beam-like) and 2-D (plate-like) structures respectively. Their manufacture and construction are also repetitive, and this leads to cost effective design solutions in a variety of mechanical, civil and aerospace engineering applications. Surveys of their dynamic and static analysis have been provided by Noor (1988), Li and Benaroya (1992), and Mead (1996).

A general classification of the known approaches for analyzing repetitive lattice structures was proposed by Noor (1988) to include four classes, namely: direct, discrete field, periodic structure and substitute continuum methods. The method presented in this paper is a development of the second of these, which was

* Corresponding author. Tel.: +44-23-8059-7664; fax: +44-23-8059-4813.
E-mail address: ekarpov@mech.soton.ac.uk (E.G. Karpov).

0020-7683/02/$ - see front matter © 2002 Published by Elsevier Science Ltd.
PII: S0020-7683(02)00259-7

defined by Dean (1976) as "The term discrete field analysis denotes the body of concepts used to obtain *field* or *functional solutions* for systems most accurately represented as a lattice or a pattern of elements". The basic idea of the approach is to take advantage of geometrical regularity of the lattice and to write equilibrium and compatibility equations for a typical joint as a set of simultaneous finite difference equations. The position of the joint in the structure is defined by one or several (for multi-dimensional lattices) independent parameters—discrete spatial coordinates—and the corresponding solutions for the governing equations are viewed as discrete vector functions of these parameters.

One of the first discrete field analyses for regular lattices was presented by Ellington and McCallion (1957), where the authors derived and solved a set of functional governing equations for a rectangular grid under out-of-plane static loadings. During the next two decades, numerous contributions to the area were made by Dean, including a monograph (1976) and "state-of-the-art" report (1975), Dean and Avent. In terms of computational effort, the use of final functional solutions for the purposes of further stress, buckling and other analyses is essentially cheaper than employing the conventional direct techniques (see, for example, the works by Dean and Jetter (1972), Issa and Avent (1991), and Renton (1973)). However, the procedures for developing and solving the governing finite difference equations "can be substantial for complex lattice configurations" (Noor, 1988). Later, Avent et al (1991) proposed the compact matrix form of the governing equations, $\mathbf{K}_n\mathbf{d}(n) = \mathbf{f}(n)$, where $\mathbf{K}_n$ is the matrix constructed from the finite difference operators relating to the structural stiffness properties, $\mathbf{f}(n)$ and $\mathbf{d}(n)$ are the given joint loading and the sought joint displacement vectors as functions of the discrete spatial parameter n. However, each entry to the matrix $\mathbf{K}_n$ served there as a separate operator that had to be assembled individually according to the type of a lattice under consideration and the boundary conditions. In the present paper, we set up the alternative governing equation as the *operator form*, $\widehat{\mathbf{K}}\mathbf{d} = \mathbf{f}$, where $\widehat{\mathbf{K}}$ is a single physical *stiffness operator* with a functional matrix kernel $\mathbf{K}$. This form is initially written regardless of the boundary conditions, therefore the kernel relates solely to the lattice geometric and material properties. Moreover, the regularity of the lattice bar arrangement implies spatial invariance of the kernel (i.e., invariance in respect of the values of spatial parameters), and the action of the stiffness operator, for *any* repetitive lattice, can be reduced to a discrete convolution sum over the kernel and displacement functions. At the same time, the required values of $\mathbf{K}$ can be easily determined from the stiffness matrix of the *associate* substructure—a minimum set of structural elements interacting with one typical nodal set of the lattice.

The convolution form of the governing equation suggests effective solution by a transform method, specifically by the discrete Fourier transform (DFT). Recent applications of DFT to the static analysis of repetitive structures were made by Ryvkin et al. (1999) who considered the problem of optimal design of *infinite* repetitive beam-like frameworks, and Moses et al. (2001) who outlined a general methodology for the static analysis of infinite periodic structures. The case of *finite* beam-like repetitive structures was studied earlier by Samartin (1988) who employed a traditional matrix form of the governing equation. The boundary conditions were modelled there by introducing additional stiffness submatrices to convert the global stiffness matrix into a block-circulant form. These submatrices were found from the boundary conditions, and inversion of the resulting stiffness matrix was reduced to separate inversion of the decoupled blocks in the Fourier domain. In the present paper, we continue discussing the use of DFT for finite structures analysis. However, we advocate the use of the functional operator form of governing equation, Green's function solutions, and propose the virtual load and substructure technique of simulating periodic boundary conditions for lattice structures. Besides, a detailed consideration is given to the problem of eliminating singularity related to the rigid-body motion, and extension of the methodology to the case of 2-D (plate-like) lattices is demonstrated.

Despite widespread application to problems of digital signal processing (see, for example, Damper, 1995; Dudgeon and Mersereau, 1984), Fourier transform methods have received comparatively little attention in structural mechanics. The reasons why are well described by Bracewell (1986, p. 4). In short, "the response of a system to harmonic input is itself harmonic, at the same frequency, under two conditions: linearity and time invariance of the system properties''. In turn, these two properties can be restated as one: ''that the response shall be related to the stimulus by convolution''; it is the latter operation of convolution that Bracewell regards as the central unifying concept behind such transform methods. While time-invariance is commonplace, space-invariance (or translation symmetry) is less so. As Bracewell remarks ''Failure of this condition is the reason that bridge deflections are not studied by analyzing the load distribution into sinusoidal components (space harmonics)''. Obviously, a finite repetitive structure is not space-invariant, since any translation in space will cause the structure to overstep its boundary and so become distinguishable from its original configuration. However, one can utilize the spatial invariance of the *mathematical formulation only*: with certain provisos, the form of governing equation may not depend, at least formally, on values of the spatial parameters throughout the structure. Indeed, geometric regularity of a repetitive lattice implies that the form of the governing equation may vary only at the lattice boundaries. Further we can assume *formal* invariance of the stiffness operator and its kernel at the boundary locations. This can be achieved by modifying the lattice with a virtual interlayer to provide stiffness coupling between the boundary nodal locations equivalent to the coupling existing between adjacent nodal locations inside the lattice. This procedure can be also viewed as the original lattice becoming a part of a larger cyclically periodic domain; that was first outlined by Nuller (1981) to consider deformation of multi-layered continuous plates. The physical effect of the virtual interlayer can be eliminated by introducing additional compensating forces to satisfy the boundary and force equilibrium conditions. Thus, the required spatial invariance of mathematical formulation can be achieved even for a finite structure. The kernel, load and displacement functions may be then viewed as periodic sequences defined for the modified lattice, and the DFT becomes an effective tool to seek the solution as a superposition of space harmonics.

The method logically simplifies for the particular case of *periodic* or *Born–von Kármán* boundary conditions. The imposition of these conditions to structural systems was well described by Keane and Price (1989), and more recently by Langley (1997). In this case, no virtual interlayer is required to provide the formal equivalence of internal and boundary nodal locations, the compensating forces are not introduced, and the displacement solutions can be immediately written in terms of the corresponding Green's function.

The approach is developed first in the context of a 1-D setting, and then extended to the 2-D case; in Section 4, several examples are given to demonstrate its practical use.

2. Beam-like structures

2.1. Boundary value problem definition. Convolution form of the governing equation

As focus for discussion, consider the planar truss, Fig. 1(a), presumed fixed in some as yet unspecified manner. Isolate mentally a minimum set of nodes, which generates the rest of the structural joints if translated along the axial direction of the beam to some equidistant spatial locations numbered as $n = 0, 1, 2, \dots, N$. We call such a set of joints the *typical* (*repeating*) nodal location or nodal set, and define the *associate* substructure as consisting of all the structural bar-elements that interact with the joints of one typical set; see Fig. 1(b) and (c).

The associate substructure stiffness matrix can be found by conventional means to give a 3×3 block form, where the three medial submatrices may be denoted $\mathbf{K}(1)$, $\mathbf{K}(0)$ and $\mathbf{K}(-1)$ to give static equilibrium in the form:

$$\begin{pmatrix} \cdots & \cdots & \cdots \\ \mathbf{K}(1) & \mathbf{K}(0) & \mathbf{K}(-1) \\ \cdots & \cdots & \cdots \end{pmatrix} \begin{pmatrix} \mathbf{d}(n-1) \\ \mathbf{d}(n) \\ \mathbf{d}(n+1) \end{pmatrix} = \begin{pmatrix} \mathbf{f}(n-1) \\ \mathbf{f}(n) \\ \mathbf{f}(n+1) \end{pmatrix}. \tag{1}$$

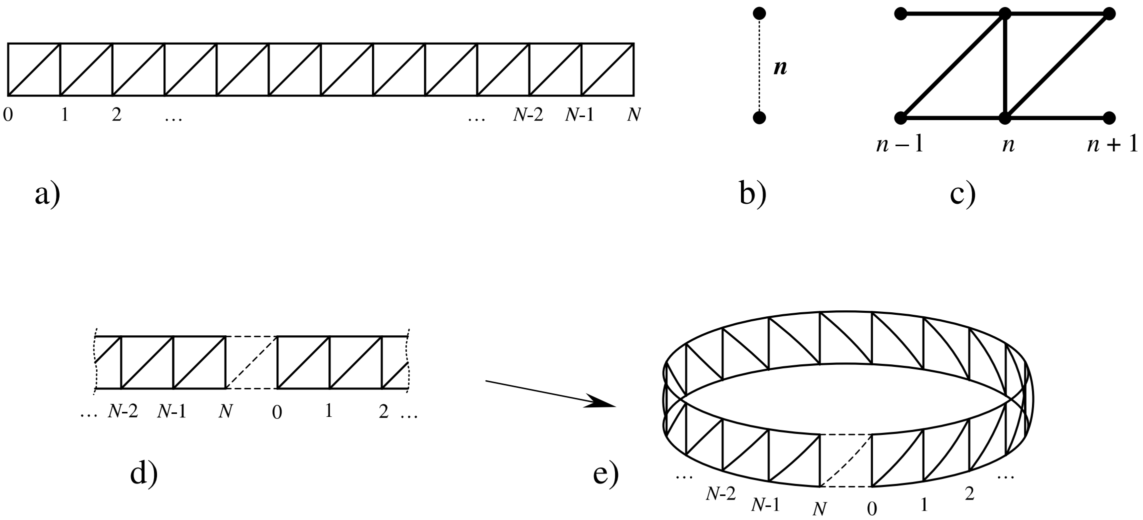

Fig. 1. Repetitive beam-like truss (a); typical nodal location (b) and associate substructure (c). Visualization of the formal coupling between boundary nodal locations (d), and closure into $(N+1)$-periodic cyclic structure (e).

Here, the column-vectors of the generalized loads and displacements, $\mathbf{f}(n)$ and $\mathbf{d}(n)$, are associated with degrees of freedom of the nodes at the corresponding spatial locations. Physically, block $\mathbf{K}(0)$ relates to the stiffness of the entire associate substructure, and blocks $\mathbf{K}(1)$, $\mathbf{K}(-1)$ are responsible for the right- and left-hand stiffness coupling between the adjacent nodal locations. Then, for any location $n = 1, 2, \ldots, N-1$, we can write:

$$\mathbf{K}(1)\mathbf{d}(n-1) + \mathbf{K}(0)\mathbf{d}(n) + \mathbf{K}(-1)\mathbf{d}(n+1) = \mathbf{f}(n). \tag{2}$$

This second order finite difference scheme represents the *governing equation* of static equilibrium of an arbitrary repetitive beam-like lattice. It can be reduced to the operator form,

$$\widehat{\mathbf{K}}\mathbf{d} = \mathbf{f}. \tag{3}$$

This representation implies that the operator $\widehat{\mathbf{K}}$ acts on the entire vector function $\mathbf{d}$, not only on a specific vector assigned by $\mathbf{d}(n)$. $\widehat{\mathbf{K}}$ is the *stiffness operator* for the lattice, which carries a functional matrix kernel $\mathbf{K}(n-n')$ and acts as a discrete convolution summation,

$$\sum_{n'=n-1}^{n+1} \mathbf{K}(n-n')\mathbf{d}(n') = \mathbf{f}(n), \qquad n = 1, 2, \ldots, N-1, \quad \mathbf{d}(0),\ \mathbf{d}(N). \tag{4}$$

The solution $\mathbf{d}(n)$ for Eq. (2) or (4) is a vector function of the discrete parameter n that fully describes some equilibrium state of the static deformation occurring in the beam in response to an external load pattern, assigned by the function $\mathbf{f}(n)$, and boundary conditions $\mathbf{d}(0)$, $\mathbf{d}(N)$. Function $\mathbf{d}(n)$ can be termed, therefore, the displacement *state function*, whereas expression (4) represents the boundary value problem for finding $\mathbf{d}(n)$ at $n = 1, 2, \ldots, N-1$.

Eq. (4) may be rewritten symbolically, employing the symbol $*$ for the convolution, as

$$\mathbf{K} * \mathbf{d} = \mathbf{f}, \tag{5}$$

and can be treated by employing a transform method that converts the operation of convolution into ordinary matrix multiplication in the transformed domain; an adaptation of the DFT method for solving

(4) and (5) will be described in the Section 2.2. In general, the state function will consist of two parts: a particular solution of the inhomogeneous form (4) and (5), pertaining to a given external load $\mathbf{f}(n)$, and a solution to the homogeneous equation

$$\mathbf{K} * \mathbf{d} = \mathbf{0} \tag{6}$$

($\mathbf{0}$ is the zero vector), relating to the trivial load, $\mathbf{f}(n) = \mathbf{0}$ for all n.

2.2. Discrete Fourier transform method

2.2.1. The (N + 1)-periodic lattice

By definition, the DFT is performed over infinite *periodic* sequences (see, for example, Damper, 1995). To satisfy this requirement we formally extend the definition intervals of functions $\mathbf{d}(n)$, $\mathbf{f}(n)$ and $\mathbf{K}(n)$ in the $(N+1)$-periodic way:

$$\begin{aligned} &\mathbf{d}(n + v(N+1)) \triangleq \mathbf{d}(n), \quad \mathbf{f}(n + v(N+1)) \triangleq \mathbf{f}(n), \quad \mathbf{K}(n + v(N+1)) \triangleq \mathbf{K}(n), \\ &n = 0, 1, 2, \ldots, N, \quad v = 0, \pm 1, \pm 2, \ldots. \end{aligned} \tag{7}$$

Then the validity of (4) for $n = 1, 2, \ldots, N-1$ implies also that it holds for all the periodically corresponding values of this parameter, $n + v(N+1)$. Moreover, the periodicity of the kernel function would mean the validity of the governing equation (4) at the boundary nodal locations, $n = 0$, N, as well. Indeed, the $(N+1)$-periodic kernel $\mathbf{K}(n)$ with non-trivial values $\mathbf{K}(0)$ and $\mathbf{K}(\pm 1)$ will yield also non-zero $\mathbf{K}(-N) = \mathbf{K}(1)$ and $\mathbf{K}(N) = \mathbf{K}(-1)$ to formally imply the stiffness coupling between the boundary locations:

$$\begin{aligned} &\mathbf{K}(-N)\mathbf{d}(N) + \mathbf{K}(0)\mathbf{d}(0) + \mathbf{K}(-1)\mathbf{d}(1) = \mathbf{f}(0), \\ &\mathbf{K}(1)\mathbf{d}(N-1) + \mathbf{K}(0)\mathbf{d}(N) + \mathbf{K}(N)\mathbf{d}(0) = \mathbf{f}(N). \end{aligned} \tag{8a}$$

Here, $\mathbf{f}(0)$ and $\mathbf{f}(N)$ are as yet unknown boundary loads that will be discussed below. With the use of periodic extension for functions $\mathbf{d}(n)$ and $\mathbf{K}(n)$, Eq. (8a) can be rewritten as

$$\begin{aligned} &\mathbf{K}(1)\mathbf{d}(-1) + \mathbf{K}(0)\mathbf{d}(0) + \mathbf{K}(-1)\mathbf{d}(1) = \mathbf{f}(0), \\ &\mathbf{K}(1)\mathbf{d}(N-1) + \mathbf{K}(0)\mathbf{d}(N) + \mathbf{K}(-1)\mathbf{d}(N+1) = \mathbf{f}(N), \end{aligned} \tag{8b}$$

which is identical with (4) for $n = 0$ and N. The coupling (8a) is shown in Fig. 1(d). It is symbolized there by modifying the lattice with a virtual substructure, which represents the bar-elements, interconnecting two neighbouring nodal sets, and formally provides the required continuity at the ends of the lattice. The periodicity of functions (7), defined for the modified lattice, may be then visualised by closing the structure to form the ring depicted in Fig. 1(e).

Thus we have converted the original boundary value problem for a repetitive beam-like lattice discussed in the comments to Eq. (4), into the mathematically equivalent problem for the modified cyclic structure shown in Fig. 1e. There are given:

(a) Eq. (4), which is valid for $n = 0, 1, \ldots, N$,
(b) the displacement vectors $\mathbf{d}(0)$ and $\mathbf{d}(N)$,
(c) the external loads $\mathbf{f}(n)$ at $n = 1, 2, \ldots, N-1$;

and we seek to find:

(a) the boundary loads $\mathbf{f}(0)$ and $\mathbf{f}(N)$,
(b) the displacements $\mathbf{d}(n)$ at $n = 1, 2, \ldots, N-1$.

The advantage of this problem formulation is the uniformity of the convolutional coupling in Eq. (4) for *all* n, including $n = 0$ and N. This allows one to treat the problem with the use of DFTs in a very natural way.

It is important to note that the boundary force reactions (left side of (8b)) are given by two components: reactions of the actual and virtual substructures, i.e.

$$\mathbf{f}^{(\mathrm{a})}(0) + \mathbf{f}^{(\mathrm{v})}(0) = \mathbf{f}(0), \qquad \mathbf{f}^{(\mathrm{a})}(N) + \mathbf{f}^{(\mathrm{v})}(N) = \mathbf{f}(N), \tag{8c}$$

as opposed to the non-boundary reactions, for which we can write simply

$$\mathbf{f}^{(\mathrm{a})}(n) = \mathbf{f}(n), \quad n = 1, 2, \ldots, N-1. \tag{8d}$$

Since only the actual addends of the load vectors $\mathbf{f}(0)$ and $\mathbf{f}(N)$ are physically present, the virtual terms can be viewed as additional compensating forces, which would *eliminate* the effect of virtual interlayer, if the modified lattice solution satisfied the original beam boundary conditions. Then the equivalence of static solutions for the original and modified problems can be achieved. For a boundary value problem (4) with specified displacements $\mathbf{d}(0)$ and $\mathbf{d}(N)$, the *resultant* vectors $\mathbf{f}(0)$ and $\mathbf{f}(N)$ can be found at once, as will be described in Section 2.2.4. However, for problems with partially specified boundary displacements, when the corresponding (actual) boundary forces are given instead, the unknown actual and virtual components of vectors (8c) have to be evaluated *separately* by employing boundary conditions (4) and also—the stiffness matrix relationship for the virtual substructure (Example 4.3, Section 4).

2.2.2. Particular non-homogeneous solution and the Green's function

Apply the finite DFT to both sides of Eq. (4), where functions $\mathbf{d}(n)$, $\mathbf{f}(n)$ and $\mathbf{K}(n-n')$ possess the properties (7) and (8a),

$$\sum_{n=0}^{N} \sum_{n'=n-1}^{n+1} \mathbf{K}(n-n')\mathbf{d}(n')\mathrm{e}^{-\mathrm{i}2\pi p \frac{n}{N+1}} = \sum_{n=0}^{N} \mathbf{f}(n)\mathrm{e}^{-\mathrm{i}2\pi p \frac{n}{N+1}}. \tag{9}$$

Then multiply and divide the left-hand side of (9) by $\mathrm{e}^{-\mathrm{i}2\pi p(n'/(N+1))}$, introduce parameter $s = n - n'$, and rearrange to give

$$\sum_{n=0}^{N} \sum_{n'=n-1}^{n+1} \mathbf{K}(n-n')\mathrm{e}^{-\mathrm{i}2\pi p \frac{n-n'}{N+1}} \mathbf{d}(n')\mathrm{e}^{-\mathrm{i}2\pi p \frac{n'}{N+1}} = \sum_{s=-1}^{1} \mathbf{K}(s)\mathrm{e}^{-\mathrm{i}2\pi p \frac{s}{N+1}} \sum_{n=0}^{N} \mathbf{d}(n-s)\mathrm{e}^{-\mathrm{i}2\pi p \frac{n-s}{N+1}}. \tag{10}$$

Due to the $(N+1)$-periodicity of $\mathbf{d}(n)$,

$$\sum_{n=0}^{N} \mathbf{d}(n-s)\mathrm{e}^{-\mathrm{i}2\pi p \frac{n-s}{N+1}} = \sum_{n=0}^{N} \mathbf{d}(n)\mathrm{e}^{-\mathrm{i}2\pi p \frac{n}{N+1}} \tag{11}$$

for any integer s. Therefore we can introduce the Fourier images of functions (7) as

$$\begin{aligned} \mathbf{D}(p) &\triangleq \sum_{n=0}^{N} \mathbf{d}(n)\mathrm{e}^{-\mathrm{i}2\pi p \frac{n}{N+1}}, \\ \mathbf{F}(p) &\triangleq \sum_{n=0}^{N} \mathbf{f}(n)\mathrm{e}^{-\mathrm{i}2\pi p \frac{n}{N+1}}, \\ \mathbf{Q}_{N+1}(p) &\triangleq \sum_{n-n'=0,\pm 1} \mathbf{K}(n-n')\mathrm{e}^{-\mathrm{i}2\pi p \frac{n-n'}{N+1}}, \end{aligned} \tag{12}$$

and write the transformed (p-domain) governing equation, according to (9)–(11), in the form

$$\mathbf{Q}_{N+1}(p)\mathbf{D}(p) = \mathbf{F}(p), \quad p = 0, 1, 2, \ldots, N. \tag{13}$$

Assume the matrix $\mathbf{Q}_{N+1}(p)$ is invertible for all values of p; then the p-domain solution reads

$$\mathbf{D}(p) = \mathbf{Q}_{N+1}^{-1}(p)\mathbf{F}(p), \tag{14}$$

and application of the inverse DFT to (14) yields the sought n-domain solution in the form

$$\mathbf{d}(n) = \frac{1}{N+1}\sum_{p=0}^{N}\mathbf{D}(p)\mathrm{e}^{\mathrm{i}2\pi p\frac{n}{N+1}} = \frac{1}{N+1}\sum_{p=0}^{N}\mathbf{Q}_{N+1}^{-1}(p)\mathbf{F}(p)\mathrm{e}^{\mathrm{i}2\pi p\frac{n}{N+1}}. \tag{15}$$

Further, we substitute the Fourier image $\mathbf{F}(p)$ into this equation, employing $n = n'$ for (12) to distinguish the summation index there from the argument of function $\mathbf{d}(n)$, and rearrange it to give

$$\mathbf{d}(n) = \frac{1}{N+1}\sum_{p=0}^{N}\mathbf{Q}_{N+1}^{-1}(p)\sum_{n'=0}^{N}\mathbf{f}(n')\mathrm{e}^{-\mathrm{i}2\pi p\frac{n'}{N+1}}\mathrm{e}^{\mathrm{i}2\pi p\frac{n}{N+1}} = \sum_{n'=0}^{N}\mathbf{G}_{N+1}(n-n')\mathbf{f}(n'), \tag{16}$$

$$\mathbf{G}_{N+1}(n-n') \triangleq \frac{1}{N+1}\sum_{p=0}^{N}\mathbf{Q}_{N+1}^{-1}(p)\mathrm{e}^{\mathrm{i}2\pi p\frac{n-n'}{N+1}}. \tag{17}$$

Here, the matrix function $\mathbf{G}_{N+1}(n-n')$ is the *Green's function* for Eq. (4) in the cyclic $(N+1)$-periodic domain. Thus a particular non-homogeneous solution to (4) is given by the convolution sum over the Green's and the load functions. The Green's function is given by the inverse DFT of the inverted Fourier image of the matrix kernel of the stiffness operator. And the *physical sense* of the Green's function, according to (16), is that, up to a rigid-body motion, the rth column of $\mathbf{G}_{N+1}(n-n')$ represents deflections of the nth nodal set caused by the rth component of a unit load vector applied to the n'th nodal location of a repetitive framework, which is formally closed to form the $(N+1)$-periodic ring. Obviously, this Green's function is invariable with respect to the boundary conditions in (4), and is defined only by the member stiffnesses and geometry of a considered lattice.

In fact, the above assumption on the invertibility of $\mathbf{Q}_{N+1}(p)$, used in (14), is not valid for $p = 0$. Indeed, due to the general properties of a structure stiffness matrix, the matrix $\mathbf{Q}_{N+1}(0) = \mathbf{K}(1) + \mathbf{K}(0) + \mathbf{K}(-1)$ always contains either zero or linear dependent columns. Then

$$\mathrm{Det}\,\mathbf{Q}_{N+1}(0) = 0, \tag{18}$$

and this will dictate the following: (i) the load $\mathbf{f}(n)$ must satisfy a self-equilibrium condition, otherwise the solution does not exist, and (ii) the term for $p = 0$ in the expression for the Green's function (16) must be corrected. Below we discuss these points in more details.

The singularity of matrix $\mathbf{Q}_{N+1}(0)$ implies that Eq. (13), for the case of $p = 0$,

$$\mathbf{Q}_{N+1}(0)\mathbf{D}(0) = \mathbf{F}(0), \tag{19}$$

has solutions only if vector $\mathbf{F}(0)$ is orthogonal to the nullspace of the conjugate and transposed matrix $\mathbf{Q}_{N+1}^{\mathrm{H}}(0)$. Here, $\mathbf{Q}_{N+1}(0)$ is real and symmetric, therefore $\mathbf{Q}_{N+1}^{\mathrm{H}}(0) = \mathbf{Q}_{N+1}(0)$. Then this requirement can be written as

$$\mathbf{Y}^{\mathrm{T}}\mathbf{F}(0) = \mathbf{0}, \tag{20}$$

where matrix $\mathbf{Y}$ is constructed from b column-vectors comprising a basis in the nullspace of matrix $\mathbf{Q}_{N+1}(0)$, and $\mathbf{0}$ is a zero-vector of dimensionality b. Note, vector $\mathbf{F}(0)$ represents, due to (12), the sum of all external nodal forces added in a translation sense around the ring,

$$\mathbf{F}(0) = \sum_{n=0}^{N} \mathbf{f}(n), \tag{21}$$

and the columns of $\mathbf{Y}$, as will be shown in Section 2.2.3, describe the structure's rigid-body motions only; therefore, (20) gives the *equilibrium condition* for external loads at the modified lattice along the global coordinate directions.

Due to the orthogonality (20), a non-trivial solution to Eq. (19) can be sought as a vector from the adjoint subspace (spanned by the eigenvectors $\mathbf{w}_r$ of $\mathbf{Q}_{N+1}(0)$ relating to its non-zero eigenvalues Λ_r):

$$\mathbf{D}(0) = \sum_{r=1}^{R-b} a_r \mathbf{w}_r, \tag{22}$$

where R is the dimensionality of the vectors in (4) and (13). Then substitute (22) into (19) to obtain

$$\mathbf{F}(0) = \mathbf{Q}_{N+1}(0) \sum_{r=1}^{R-b} a_r \mathbf{w}_r = \sum_{r=1}^{R-b} \Lambda_r a_r \mathbf{w}_r. \tag{23}$$

Further, introduce $\mathbf{W} = (\, \mathbf{w}_1 \quad \mathbf{w}_2 \quad \cdots \quad \mathbf{w}_{R-b} \,)$ as a rectangular matrix of size $R \times (R-b)$, matrix $\mathbf{\Lambda} = \mathrm{diag}\,(\Lambda_1, \Lambda_2, \ldots, \Lambda_{R-b})$ as a square matrix of size $(R-b) \times (R-b)$, and the vector $\mathbf{a} = (\, a_1 \quad a_2 \quad \cdots \quad a_{R-b} \,)^{\mathrm{T}}$. Then we may rewrite (22) and (23) as

$$\begin{aligned} \mathbf{D}(0) &= \mathbf{W}\mathbf{a}, \\ \mathbf{F}(0) &= \mathbf{W}\mathbf{\Lambda}\mathbf{a}, \end{aligned} \tag{24}$$

wherefrom

$$\mathbf{D}(0) = \mathbf{W}\mathbf{\Lambda}^{-1}\mathbf{W}^{+}\mathbf{F}(0); \tag{25}$$

here, $\mathbf{W}^{+}$ is the pseudoinverse of matrix $\mathbf{W}$. Therefore, the expression for the Green's function (17) has to be corrected, due to (15), (16) and (25), as the following:

$$\mathbf{G}_{N+1}(n-n') = \frac{1}{N+1} \sum_{p=0}^{N} \widetilde{\mathbf{G}}_{N+1}(p) \mathrm{e}^{\mathrm{i}2\pi p \frac{n-n'}{N+1}}, \tag{26a}$$

$$\widetilde{\mathbf{G}}_{N+1}(p) = \begin{cases} \mathbf{Q}_{N+1}^{-1}(p), & p > 0, \\ \mathbf{W}\mathbf{\Lambda}^{-1}\mathbf{W}^{+}, & p = 0; \end{cases} \tag{26b}$$

where the matrix function $\widetilde{\mathbf{G}}_{N+1}(p)$ serves as the Fourier image of the Green's function $\mathbf{G}_{N+1}(n-n')$ and exists for all values of p. Thus, a particular solution to (4) may be then taken in the form (16), where the Green's function is given by the expressions (26a) and (26b).

2.2.3. General solution of homogeneous equation

The general solution of the homogeneous form (6) describes deflection of the ring due to the trivial load pattern, $\mathbf{f}(n) = \mathbf{0}$, $n = 0, 1, \ldots, N$. Obviously, for any stiff lattice, this solution can be associated with the structure's rigid-body motions only (the zeroth space harmonics). Thus, the p-domain homogeneous equation,

$$\mathbf{Q}_{N+1}(p)\mathbf{D}(p) = \mathbf{0}, \tag{27}$$

obtained by applying the DFT to (6), can have non-trivial solutions only for $p = 0$, i.e.

$$\mathbf{D}(p) = \delta_{p,0}\mathbf{D}(0) = \delta_{p,0}\sum_{r=1}^{b} C_r\mathbf{y}_r \equiv \delta_{p,0}\mathbf{YC}. \tag{28}$$

Here, $\delta_{p,0}$ is the Kronecker delta, $\mathbf{y}_r$ are the basis vectors spanning the b-dimensional nullspace of matrix $\mathbf{Q}_{N+1}(0)$; the matrix $\mathbf{Y}$ is constructed of b column-vectors $\mathbf{y}_r$, and the vector $\mathbf{C}$ consists of b participation coefficients C_r. Then the n-domain solution is found by applying the inverse Fourier transform upon (28) to read

$$\mathbf{d}(n) = \frac{1}{N+1}\sum_{p=0}^{N}\mathbf{D}(p)\mathrm{e}^{\mathrm{i}2\pi p\frac{n}{N+1}} = \frac{1}{N+1}\mathbf{D}(0) = \frac{1}{N+1}\mathbf{YC}. \tag{29}$$

The constant factor $(N+1)^{-1}$ of the solution (29) can be included into the coefficients C_r, so we shall omit it henceforth. The basis vectors $\mathbf{y}_r$ relate to the rigid-body motion of the ring in $b = 2$ or 3 principal directions (for a planar and space truss respectively) of the global coordinate system. For instance, for a pin-jointed truss of the type shown in Fig. 1, one would get simply

$$\mathbf{d}(n) = (\mathbf{I} \quad \mathbf{I})^{\mathrm{T}}\mathbf{C} \equiv (1 \quad 0 \quad 1 \quad 0)^{\mathrm{T}}C_1 + (0 \quad 1 \quad 0 \quad 1)^{\mathrm{T}}C_2, \tag{30}$$

where $\mathbf{I}$ is the 2×2 identity matrix. The conditions required for evaluation of the coefficients C_r will be discussed in the next section.

The *general form* of solution for Eq. (4) can be written conventionally (for example, Kelley and Peterson, 2000), as the sum of a particular inhomogeneous and the general homogeneous solutions, which are given by the expressions (16) and (29) respectively, i.e. we finally obtain

$$\mathbf{d}(n) = \sum_{n'=0}^{N}\mathbf{G}_{N+1}(n-n')\mathbf{f}(n') + \mathbf{YC}, \quad n = 0,1,2,\ldots,N. \tag{31}$$

2.2.4. The boundary loads and vector C

As was mentioned above (the comments to formula (8c)), the boundary loads $\mathbf{f}(0)$ and $\mathbf{f}(N)$ do not represent genuine structural reaction, and have to be evaluated by analytical means. Besides, knowledge of vector $\mathbf{C}$ is also required for employing the solution form (31). To find these vectors, rearrange (31) as

$$\mathbf{d}(n) = \mathbf{G}_{N+1}(n)\mathbf{f}(0) + \mathbf{G}_{N+1}(n-N)\mathbf{f}(N) + \bar{\mathbf{d}}(n) + \mathbf{YC}, \tag{32}$$

where $\bar{\mathbf{d}}(n)$ is the known vector,

$$\bar{\mathbf{d}}(n) = \sum_{n'=1}^{N-1}\mathbf{G}_{N+1}(n-n')\mathbf{f}(n'), \tag{33}$$

and utilize the boundary conditions (4):

$$\begin{cases} \mathbf{d}(0) = \mathbf{G}_{N+1}(0)\mathbf{f}(0) + \mathbf{G}_{N+1}(-N)\mathbf{f}(N) + \bar{\mathbf{d}}(0) + \mathbf{YC}, \\ \mathbf{d}(N) = \mathbf{G}_{N+1}(N)\mathbf{f}(0) + \mathbf{G}_{N+1}(0)\mathbf{f}(N) + \bar{\mathbf{d}}(N) + \mathbf{YC}. \end{cases} \tag{34}$$

Then vectors $\mathbf{f}(0)$ and $\mathbf{f}(N)$ can be expressed through the b coefficients C_r (elements of $\mathbf{C}$) as

$$\begin{pmatrix} \mathbf{f}(0) \\ \mathbf{f}(N) \end{pmatrix} = \begin{pmatrix} \mathbf{G}_{N+1}(0) & \mathbf{G}_{N+1}(-N) \\ \mathbf{G}_{N+1}(N) & \mathbf{G}_{N+1}(0) \end{pmatrix}^{-1} \begin{pmatrix} \mathbf{d}(0) - \bar{\mathbf{d}}(0) - \mathbf{YC} \\ \mathbf{d}(N) - \bar{\mathbf{d}}(N) - \mathbf{YC} \end{pmatrix}. \tag{35a}$$

The equilibrium requirement (20) implies b additional conditions on values of these coefficients. As a result, expressions (20) and (35a) provide one with a sufficient system of linear equations for finding all the components of vectors $\mathbf{f}(0)$, $\mathbf{f}(N)$ and $\mathbf{C}$. Further, by substituting these vectors into (31), we obtain the analytical functional solution to (4) in terms of known components only. There are two important particular cases of problem (4). Assume we have $\mathbf{d}(0) = \mathbf{d}(N)$, and: (1) the N-periodic Born–von Karman ring can be obtained by directly merging the ends of the lattice, but the resultant vector $\mathbf{f}^{(a)}(0) + \mathbf{f}^{(a)}(N) = \mathbf{f}(0)$ is not known (it may contain unknown support reactions), or (2) the Born–von Karman ring still cannot be obtained (say, the merged elements would have larger than typical cross-section area, as in Example 4.1, Section 4). In both cases, the virtual interlayer is not introduced, N-periodic functions have to be used in (21) and (31), and the vector $\mathbf{f}(0)$ can be sought as

$$\mathbf{f}(0) \equiv \mathbf{f}(N) = \mathbf{G}_N^{-1}(0)\left(\mathbf{d}(0) - \sum_{n=1}^{N-1}\mathbf{G}_N(n-n')\mathbf{f}(n') - \mathbf{YC}\right). \tag{35b}$$

If vector $\mathbf{f}(0)$ is known in advance for the first of these cases (for some symmetric problem, for example, $\mathbf{f}^{(a)}(0) = -\mathbf{f}^{(a)}(N)$, so that $\mathbf{f}(0) = \mathbf{0}$), then a knowledge of $\mathbf{d}(0)$ is not required, and, up to a rigid-body displacement, the solution is immediately given by formula (16), where index N is to be replaced with $N-1$.

3. Plate-like structures

3.1. 2-D Boundary value problem definition

The proposed approach can be extended to the case of multi-dimensional lattices, i.e., when two or three independent parameters are required to define the location of a repeating nodal set inside the lattice. In this paper, we discuss 2-D, or "plate-like" structures only.

The typical nodal location (n, m) of a plate-like lattice is defined to comprise a minimal set of nodes, such that, if translated along the orthogonal directions of the x- and y-coordinate axes, would cover the rest of the structural joints; and the associate substructure consists then of all the structural elements interacting with the nodes of one typical set (n, m). An illustrative example is shown in Fig. 2(a) and (b), where a single node gives the repeating nodal pattern of a square cell grid; further examples (Figs. 4–6) will be considered in Section 4.

The equation of static equilibrium for the 2-D lattices can be written similarly, by considering the associate substructure stiffness matrix arranged to an appropriate block form, wherefrom, one generally obtains

$$\begin{aligned}\mathbf{f}(n,m) = {} & \mathbf{K}(1,1)\mathbf{d}(n-1,m-1) + \mathbf{K}(0,1)\mathbf{d}(n,m-1) + \mathbf{K}(-1,1)\mathbf{d}(n+1,m-1) \\ & + \mathbf{K}(1,0)\mathbf{d}(n-1,m) + \mathbf{K}(0,0)\mathbf{d}(n,m) + \mathbf{K}(-1,0)\mathbf{d}(n+1,m) \\ & + \mathbf{K}(1,-1)\mathbf{d}(n-1,m+1) + \mathbf{K}(0,-1)\mathbf{d}(n,m+1) + \mathbf{K}(-1,-1)\mathbf{d}(n+1,m+1).\end{aligned} \tag{36}$$

Here, vector functions $\mathbf{f}(n, m)$ and $\mathbf{d}(n, m)$ are the load and displacement functions of the two discrete spatial parameters respectively, and the matrix function $\mathbf{K}(n-n', m-m')$ is the 2-D kernel of the stiffness operator (3). The value $\mathbf{K}(0, 0)$ of the kernel is determined from the stiffness properties of the entire associate substructure, while the remaining values describe the stiffness coupling between adjacent nodal locations (n, m) and (n', m'). If the coupling between some of the neighbouring locations is absent (as, for instance, between the nodes (n, m) and $(n-1, m+1)$ of the grid, Fig. 2), then the corresponding value of the kernel reads a zero matrix of size R, the dimensionality of the displacement and load vectors in (36).

The second order partial finite difference equation (36) can be reduced to the *double* convolution sum over the kernel and displacement functions:

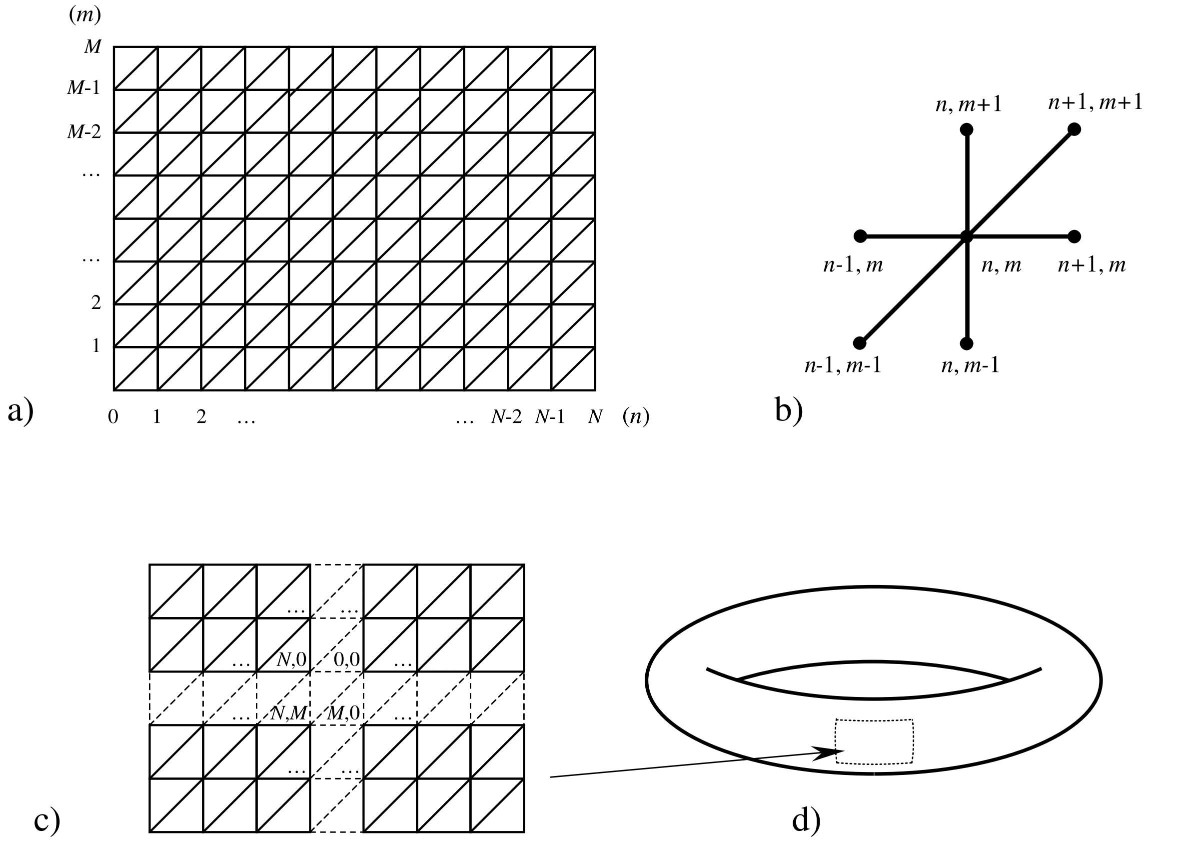

Fig. 2. Square cell grid (a) and its associate substructure (b). Formal coupling between the opposite edges of the grid (c) and closure into $(N+1, M+1)$-periodic torus (d).

$$\sum_{n'=n-1}^{n+1}\sum_{m'=m-1}^{m+1}\mathbf{K}(n-n', m-m')\mathbf{d}(n', m') = \mathbf{f}(n,m), \qquad n = 1,2,\ldots,N-1, \quad m = 1,2,\ldots,M-1. \tag{37a}$$

Provided that the 2-D boundary conditions,

$$\mathbf{d}(n,0), \quad \mathbf{d}(n,M), \quad \mathbf{d}(0,m), \quad \mathbf{d}(N,m), \qquad n = 0,1,\ldots,N, \quad m = 0,1,\ldots,M, \tag{37b}$$

are known, the above represents the boundary value problem for a plate-like lattice. The solution $\mathbf{d}(n,m)$ describes the response of the lattice to a given pattern of static external loads, assigned by the function $\mathbf{f}(n,m)$, as regards the boundary conditions (37b).

3.2. 2-D discrete Fourier transform method

3.2.1. Particular non-homogeneous solution and the 2-D Green's function

Employing 2-D DFT for solving (37a), we assume formally that the displacement, load and kernel functions are "rectangular" periodic, i.e., for $\mathbf{d}(n,m)$:

$$\mathbf{d}(n+v(N+1),m)=\mathbf{d}(n,m+w(M+1))=\mathbf{d}(n,m),$$
$$n=0,1,\ldots,N,\quad m=0,1,\ldots,M,\quad v=0,\pm1,\pm2,\ldots,\quad w=0,\pm1,\pm2,\ldots \tag{38}$$

This is required according to traditional theory (for example, Dudgeon and Mersereau, 1984) and, for the case of $\mathbf{d}(n,m)$ and $\mathbf{f}(n,m)$, does not amend the original problem definition. However, the periodicity of the kernel $\mathbf{K}(n-n',m-m')$, similar to the 1-D case, would imply the validity of the governing equation (37a) at the edges of the structure, i.e. at all the boundary nodes $(n,0)$, (n,N), $(0,m)$ and (N,m). Therefore, the structure has to be formally modified with a virtual interlayer providing the same coupling between the boundary nodal locations as exists between the internal nodes see Fig. 2(c). The procedure may be symbolized by closing the lattice into the conceptual torus, as depicted in Fig. 2(d).

By applying the 2-D DFT to Eq. (37a) we obtain the transform domain relationship

$$\mathbf{Q}_{N+1,M+1}(p,q)\mathbf{D}(p,q)=\mathbf{F}(p,q) \tag{39}$$

where the convolution sum has been replaced by ordinary matrix multiplication, and the 2-D Fourier images of displacement, load, and kernel functions are defined accordingly as

$$\begin{aligned}
&\mathbf{D}(p,q)\triangleq\sum_{n=0}^{N}\sum_{m=0}^{M}\mathbf{d}(n,m)\mathrm{e}^{-\mathrm{i}2\pi\left(p\frac{n}{N+1}+q\frac{m}{M+1}\right)},\\
&\mathbf{F}(p,q)\triangleq\sum_{n=0}^{N}\sum_{m=0}^{M}\mathbf{f}(n,m)\mathrm{e}^{-\mathrm{i}2\pi\left(p\frac{n}{N+1}+q\frac{m}{M+1}\right)},\\
&\mathbf{Q}_{N+1,M+1}(p,q)\triangleq\sum_{n'=n-1}^{n+1}\sum_{m'=m-1}^{m+1}\mathbf{K}(n-n',m-m')\mathrm{e}^{-\mathrm{i}2\pi\left(p\frac{n-n'}{N+1}+q\frac{m-m'}{M+1}\right)}.
\end{aligned} \tag{40}$$

Then the transformed domain solution reads

$$\mathbf{D}(p,q)=\mathbf{Q}_{N+1,M+1}^{-1}(p,q)\mathbf{F}(p,q). \tag{41}$$

Further application of the inverse 2-D DFT and introduction of the 2-D Green's function,

$$\mathbf{G}_{N+1,M+1}(n-n',m-m')\triangleq\frac{1}{(N+1)(M+1)}\sum_{p=0}^{N}\sum_{q=0}^{M}\mathbf{Q}_{N+1,M+1}^{-1}(p,q)\mathrm{e}^{\mathrm{i}2\pi\left(p\frac{n-n'}{N+1}+q\frac{m-m'}{M+1}\right)}, \tag{42}$$

provide a particular non-homogeneous solution in the form of the double convolution sum,

$$\mathbf{d}(n,m)=\sum_{n'=0}^{N}\sum_{m'=0}^{M}\mathbf{G}_{N+1,M+1}(n-n',m-m')\mathbf{f}(n',m'), \tag{43}$$

Here, the edge load functions,

$$\mathbf{f}(n,0),\quad \mathbf{f}(n,M),\quad \mathbf{f}(0,m),\quad \mathbf{f}(N,m),\qquad n=0,1,\ldots,N,\quad m=1,2,\ldots,M-1, \tag{44}$$

not specified originally by the problem definition (37a) and (37b), can be found by employing the boundary conditions as will be discussed later. The physical sense of the 2-D Green's function reads: up to a rigid-body motion, the rth column of $\mathbf{G}_{N+1,M+1}(n-n',m-m')$ represents deflections of nodes at the location (n,m) due to the rth component of a unit load vector applied to the location (n',m') of a plate-like lattice, which is conceptually closed to form the $(N+1,M+1)$-periodic torus.

3.2.2. Final solution form. Computational effectiveness of the approach

Using arguments similar to the 1-D case, we build the general solution of the homogeneous equation,

$$\sum_{n'=n-1}^{n+1}\sum_{m'=m-1}^{m+1}\mathbf{K}(n-n',m-m')\mathbf{d}(n',m')=\mathbf{0}, \tag{45}$$

as the following:

$$\mathbf{d}(n,m)=\sum_{r=1}^{b}C_r\mathbf{y}_r=\mathbf{YC}. \tag{46}$$

Here, $\mathbf{y}_r$ are eigenvectors of the matrix $\mathbf{Q}_{N+1,M+1}(0,0)$ relating to the zero eigenvalues and describing therefore the rigid-body displacements of the entire lattice; b is the dimensionality of the lattice ($b=2$ for planar, or 3 for space structures); C_r are arbitrary participation coefficients; matrix $\mathbf{Y}$ and vector $\mathbf{C}$ are constructed from the individual elements $\mathbf{y}_r$ and C_r respectively.

The singularity of $\mathbf{Q}_{N+1,M+1}(0,0)$ implies that the expression for the 2-D Green's function (42) has to be corrected to read

$$\begin{aligned}&\mathbf{G}_{N+1,M+1}(n-n',m-m')=\frac{1}{(N+1)(M+1)}\sum_{p=0}^{N}\sum_{q=0}^{M}\widetilde{\mathbf{G}}_{N+1,M+1}(p,q)\mathrm{e}^{\mathrm{i}2\pi\left(p\frac{n-n'}{N+1}+q\frac{m-m'}{(M+1)}\right)},\\&\widetilde{\mathbf{G}}_{N+1,M+1}(p,q)=\begin{cases}\mathbf{Q}^{-1}_{N+1,M+1}(p,q), & p+q>0,\\ \mathbf{W}\boldsymbol{\Lambda}^{-1}\mathbf{W}^{+}, & p=q=0.\end{cases}\end{aligned} \tag{47}$$

Here, $\widetilde{\mathbf{G}}_{N+1,M+1}(p,q)$ is the 2-D Fourier image of the Green's function, and the matrices

$$\boldsymbol{\Lambda}=\mathrm{diag}\,(\Lambda_1,\Lambda_2,\ldots,\Lambda_{R-b}),\qquad \mathbf{W}=(\,\mathbf{w}_1\quad\mathbf{w}_2\quad\cdots\quad\mathbf{w}_{R-b}\,) \tag{48}$$

are respectively constructed from the non-zero eigenvalues and the corresponding eigenvectors of the matrix $\mathbf{Q}_{N+1,M+1}(0,0)$.

Summarising the above results, we write the general solution to (37a) in the form

$$\mathbf{d}(n,m)=\sum_{n'=0}^{N}\sum_{m'=0}^{M}\mathbf{G}_{N+1,M+1}(n-n',m-m')\mathbf{f}(n',m')+\mathbf{YC},\qquad n=0,1,\ldots,N,\quad m=0,1,\ldots,M, \tag{49}$$

where the boundary loads (44) and the vector $\mathbf{C}$ can be found by employing the equilibrium requirement,

$$\mathbf{Y}^{\mathrm{T}}\mathbf{F}(0,0)\equiv\mathbf{Y}^{\mathrm{T}}\sum_{n=0}^{N}\sum_{m=0}^{M}\mathbf{f}(n,m)=\mathbf{0}, \tag{50}$$

and boundary conditions (37b). Indeed, by substituting (37b) to (49) we can express the edge load vectors (44) through the b components of vector $\mathbf{C}$ for all the required values of parameters n and m. Further substitution of these vectors into (50) gives b equations to determine the coefficients C_r; so that one can finally rewrite solution (49) in terms of only known components.

Similar to the 1-D case (see the comments to equation (35b)), the task of finding the boundary loads can be simplified, when less than four functions (37b) are required to specify displacements along the boundary line of lattice; i.e. when we can write $\mathbf{d}(n,0)=\mathbf{d}(n,M)$, $n=0,1,\ldots,N$, or/and $\mathbf{d}(0,m)=\mathbf{d}(N,m)$, $m=0,1,\ldots,M$ (Examples 4.4–4.6, Section 4). In these cases, the periodicity of functions in (49) and (50) reduces to $(N,M+1)$, $(N+1,M)$ or (N,M) accordingly, and introduction of functions $\mathbf{f}(n,M)$ and/or

$\mathbf{f}(N, m)$ is not required; that will considerably reduce computational efforts for finding the boundary loads around the lattice. The situation of mixed boundary conditions, when actual parts of boundary loads are given instead of displacements at some areas along the lattice edge, is also similar to the beam-like case. The unknown actual and virtual components of vectors (44) then have to be evaluated separately by employing both the known boundary conditions and the force–displacement relationship (stiffness matrix) for the virtual interlayer (Example 4.4, Section 4).

The tasks of finding the boundary loads, parametric inversion of matrix $\mathbf{Q}_{N+1,M+1}(p, q)$ and further calculation of the Green's functions (47) contribute most to the overall computational cost of this approach. It is noteworthy that the last two of these have to be performed once only for a given lattice, and the cost of the parametric inversion does not depend on the size of lattice. The standard algorithms for matrix inversion (for solving $\mathbf{Ax} = \mathbf{b}$) requires $\sim n^3$ processes, Strang (1988), where n is the order of the matrix. The cost of the present method can be then estimated as $\sim(N + M)^3 + (NM)^2$ processes—for the boundary loads and Green's function respectively, compared with $\sim(NM)^3$ processes—for the direct matrix method. For beam-like lattices this estimate is $\sim N^0 + N^2$ (the cost of boundary loads also becomes independent of the size of lattice) and $\sim N^3$. Thus, the method is most effective for the repeated analysis of a large lattice problem with varying boundary conditions and load patterns.

4. Illustrative examples

Example 4.1. For the repetitive pin-jointed plane truss shown in Fig. 3, assume L is the length of the non-diagonal bars; E and A are Young's modulus and cross-section area of all bars respectively. The associate substructure of the truss is shown in Fig. 3(b). The kernel $\mathbf{K}(n - n')$ for this truss was found from the associate substructure stiffness matrix according to (1) to read

$$\mathbf{K}(1) = \frac{-EA}{2\sqrt{2}L}\begin{pmatrix} 2\sqrt{2} & 0 & 1 & 1 \\ 0 & 0 & 1 & 1 \\ 1 & -1 & 2\sqrt{2} & 0 \\ -1 & 1 & 0 & 0 \end{pmatrix}, \quad \mathbf{K}(0) = \frac{EA}{2L}\begin{pmatrix} 4+\sqrt{2} & 0 & 0 & 0 \\ 0 & 2+\sqrt{2} & 0 & -2 \\ 0 & 0 & 4+\sqrt{2} & 0 \\ 0 & -2 & 0 & 2+\sqrt{2} \end{pmatrix},$$

$$\mathbf{K}(-1) = \mathbf{K}^{\mathrm{T}}(1), \quad \text{and} \quad \mathbf{K}(n - n') = \mathbf{0} \quad \text{if } n - n' \neq 0, \pm 1. \tag{51}$$

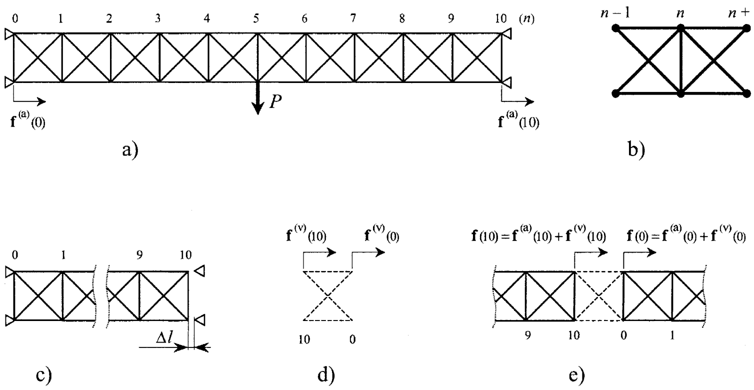

Fig. 3. Bridge deflection (a) and lack of fit (c) problems with a planar X-braced truss; associate substructure of the truss (b). Virtual interlayer (d) and the boundary loads (e).

For the bridge deflection problem, Fig. 3(a), we have

$$\mathbf{f}(n) = \delta_{n,5}(0 \quad 0 \quad 0 \quad -P)^{\mathrm{T}}, \quad n = 1, 2, \ldots, 9; \qquad \mathbf{d}(0) = \mathbf{d}(10) = \mathbf{0} \tag{52}$$

(the ends of the truss are fixed). The virtual interlayer is not required, and the N-periodic solution ($N = 10$) can be built according to (31). The unknown vectors $\mathbf{C}$ and $\mathbf{f}(0) = \mathbf{f}^{(a)}(0) + \mathbf{f}^{(a)}(10)$ must satisfy the boundary (35b) and equilibrium (20) requirements. The Fourier images of the kernel and Green's function are to be found according to (12) and (26b) respectively, where

$$\boldsymbol{\Lambda} = \frac{EA}{L}\begin{pmatrix} \sqrt{2} & 0 \\ 0 & 2+\sqrt{2} \end{pmatrix}, \quad \mathbf{W} = \begin{pmatrix} -1 & 0 & 1 & 0 \\ 0 & -1 & 0 & 1 \end{pmatrix}^{\mathrm{T}}, \quad \mathbf{Y} = \begin{pmatrix} 1 & 0 & 1 & 0 \\ 0 & 1 & 0 & 1 \end{pmatrix}^{\mathrm{T}}, \tag{53}$$

and the values of kernel are given by (51). The diagonal elements of $\boldsymbol{\Lambda}$ are the non-zero eigenvalues of matrix $\mathbf{Q}_N(0)$, the columns of $\mathbf{W}$ are the corresponding eigenvectors, and the columns of $\mathbf{Y}$ give a basis in the nullspace of $\mathbf{Q}_N(0)$. The Green's function $\mathbf{G}_N(n - n')$ is then calculated according to (26a), and the static response is given by the displacement function,

$$\begin{aligned} &\mathbf{d}(n) = \mathbf{G}_{10}(n)\mathbf{f}(0) + \mathbf{G}_{10}(n-5)\mathbf{f}(5) + \mathbf{YC}, \quad \mathbf{C} = P\frac{L}{EA}(0 \quad -6.7678)^{\mathrm{T}}, \\ &\mathbf{f}(0) = P(0 \quad 0.50444 \quad 0 \quad 0.49556)^{\mathrm{T}}, \quad n = 0, 1, \ldots, 10. \end{aligned} \tag{54}$$

Example 4.2. Now consider the lack of fit problem shown in Fig. 3(c):

$$\mathbf{f}(n) = \mathbf{0}, \quad n = 1, 2, \ldots, 9; \qquad \mathbf{d}(0) = \mathbf{0}, \quad \mathbf{d}(10) = \Delta l(1 \quad 0 \quad 1 \quad 0)^{\mathrm{T}}. \tag{55}$$

Since $\mathbf{d}(0) \neq \mathbf{d}(10)$ here, the virtual interlayer is introduced as shown in Fig. 3(d) and (e), and the $(N+1)$-periodic solution has to be built, as given by (31):

$$\begin{aligned} &\mathbf{d}(n) = \mathbf{G}_{11}(n)\mathbf{f}(0) + \mathbf{G}_{11}(n-10)\mathbf{f}(10) + \mathbf{YC}, \quad \mathbf{f}(0) = \Delta l\frac{EA}{L}(-f_x \quad -f_y \quad -f_x \quad f_y)^{\mathrm{T}}, \\ &\mathbf{f}(10) = \Delta l\frac{EA}{L}(f_x \quad -f_y \quad f_x \quad f_y)^{\mathrm{T}}, \quad f_x = 1.47533, \quad f_y = 0.32777, \quad \mathbf{C} = \Delta l(1/2 \quad 0)^{\mathrm{T}}; \end{aligned} \tag{56}$$

where the summarized end loads $\mathbf{f}(0)$, $\mathbf{f}(10)$ and vector $\mathbf{C}$ were found by using (20) and (35a).

Example 4.3. The approach for finding the end loads varies, when some of their actual components are specified instead of the corresponding boundary displacements. Assume, for instance, that

$$\mathbf{f}(n) = \mathbf{0}, \quad n = 1, 2, \ldots, 9; \quad \mathbf{d}(0) = \mathbf{0}, \quad \mathbf{f}^{(a)}(10) = (P \quad 0 \quad P \quad 0)^{\mathrm{T}}. \tag{57}$$

The virtual components of the end loads will compensate the effect of the virtual substructure (see Fig. 3(d) and (e)), if they satisfy the stiffness matrix relationship for the latter, which reads here

$$\begin{pmatrix} \mathbf{f}^{(v)}(10) \\ \mathbf{f}^{(v)}(0) \end{pmatrix} = \begin{pmatrix} \mathbf{K}_1 & \cdots \\ \mathbf{K}_2 & \cdots \end{pmatrix}\begin{pmatrix} \mathbf{d}(10) \\ \mathbf{d}(0) \end{pmatrix}, \quad \mathbf{K}_1 = \frac{EA}{2\sqrt{2}L}\begin{pmatrix} 1+2\sqrt{2} & -1 & 0 & 0 \\ -1 & 1 & 0 & 0 \\ 0 & 0 & 1+2\sqrt{2} & 1 \\ 0 & 0 & 1 & 1 \end{pmatrix}, \quad \mathbf{K}_2 = \mathbf{K}(1) \tag{58}$$

(only the left half of the virtual substructure stiffness matrix is required, since $\mathbf{d}(0) = \mathbf{0}$). This expression can be termed the *compensation* demand; if employed together with the boundary (57), equilibrium (20) conditions and formulas (8c), it gives a sufficient system of linear equations for finding all the unknown vectors $\mathbf{f}^{(a)}(0)$, $\mathbf{f}^{(v)}(0)$, $\mathbf{f}^{(v)}(10)$, $\mathbf{d}(10)$ and $\mathbf{C}$. The displacement solution then has the same form as (56), with

$$\begin{aligned} &\mathbf{f}(0) = P(-12.176 \quad -2.7322 \quad -12.176 \quad 2.7322)^{\mathrm{T}}, \\ &\mathbf{f}(10) = P(12.176 \quad -2.9438 \quad 12.176 \quad 2.9438)^{\mathrm{T}}, \end{aligned} \quad \mathbf{C} = P\frac{L}{EA}(4.1075 \quad 0)^{\mathrm{T}}. \tag{59}$$

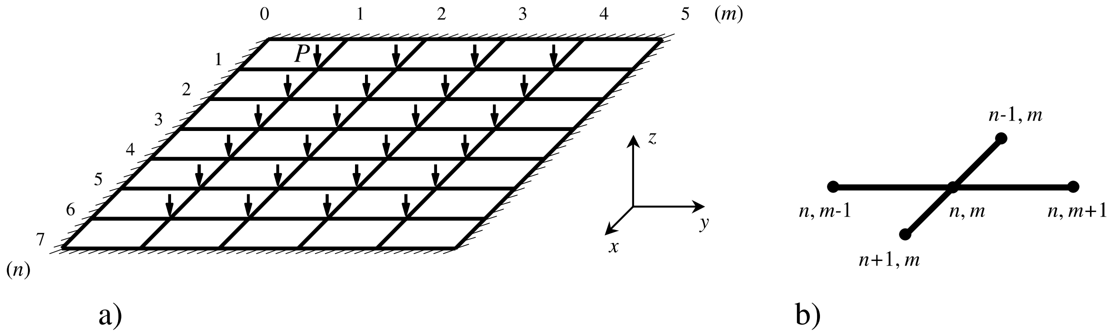

Fig. 4. Clamped grid under uniform transverse load (a). Associate substructure of the grid (b).

Example 4.4. Next consider the 2-D rigid-jointed square cell grid, which is clamped at the edges and subjected to a uniform transverse load, Fig. 4(a):

$$\mathbf{f}(n,m) = (-P \quad 0 \quad 0), \quad n = 1,2,\ldots,6, \quad m = 1,2,\ldots,4;$$
$$\mathbf{d}(n,0) = \mathbf{d}(n,5) = \mathbf{d}(0,m) = \mathbf{d}(7,m) = \mathbf{0}, \quad n = 0,1,\ldots,7, \quad m = 0,1,\ldots,5. \tag{60}$$

The repeating nodal location of the grid is represented by a single node with two rotational (in the yz- and xz-planes respectively) and one spatial degree of freedom. The associate substructure is then the crosspiece shown in Fig. 4b. The 2-D matrix kernel for this lattice has five non-trivial values given below:

$$\mathbf{K}(0,1) = \frac{E}{L^3}\begin{pmatrix} -12I & 6IL & 0 \\ -6IL & 2IL^2 & 0 \\ 0 & 0 & -GJL^2/E \end{pmatrix}, \quad \mathbf{K}(1,0) = \frac{E}{L^3}\begin{pmatrix} -12I & 0 & 6IL \\ 0 & -GJL^2/E & 0 \\ -6IL & 0 & 2IL^2 \end{pmatrix},$$
$$\mathbf{K}(0,0) = \frac{2}{L^3}\begin{pmatrix} 24EI & 0 & 0 \\ 0 & (4EI+GJ)L^2 & 0 \\ 0 & 0 & (4EI+GJ)L^2 \end{pmatrix},$$
$$\mathbf{K}(0,-1) = \mathbf{K}^{\mathrm{T}}(0,1), \quad \mathbf{K}(-1,0) = \mathbf{K}^{\mathrm{T}}(1,0) \tag{61}$$

I, J, L, E, and G are respectively the second moment of area, polar second moment of area, length, Young's and shear moduli of the individual (circular cross-section) members. Entries (61) were obtained by considering the crosspiece stiffness matrix. The Fourier image of the kernel is then found according to (40), and the matrices $\mathbf{\Lambda}$, $\mathbf{W}$ and $\mathbf{Y}$ read

$$\mathbf{\Lambda} = \frac{12EI}{L}\begin{pmatrix} 1 & 0 \\ 0 & 1 \end{pmatrix}, \quad \mathbf{W} = \begin{pmatrix} 0 & 1 & 0 \\ 0 & 0 & 1 \end{pmatrix}^{\mathrm{T}} \quad \text{and} \quad \mathbf{Y} = (1 \quad 0 \quad 0)^{\mathrm{T}} \tag{62}$$

Since $\mathbf{d}(n,0) = \mathbf{d}(n,5) = \mathbf{d}(0,m) = \mathbf{d}(7,m) = \mathbf{0}$ for all n, m, the (N,M)-periodic functions ($N = 7$, $M = 5$) can be used in the solution form (49), and only two boundary load functions, $\mathbf{f}(n,0)$ and $\mathbf{f}(0,m)$, are to be found. Assuming $J = 2I = 625/6$ mm^4, $L = 100$ mm, $E = 2.5G = 2 \times 10^5$ N/mm^2, $P = 20$ N, and using the boundary (60) and equilibrium (50) conditions, we obtain

$$\mathbf{C} = (-0.82447), \ \mathbf{f}(0,0) = \mathbf{0}, \ \mathbf{f}(1,0) = (24.611 \quad 0 \quad -887.15)^{\mathrm{T}},$$
$$\mathbf{f}(2,0) = (60.163 \quad 0 \quad -632.93)^{\mathrm{T}}, \ \mathbf{f}(3,0) = (75.895 \quad 0 \quad -207.26)^{\mathrm{T}},$$
$$\mathbf{f}(0,1) = (24.102 \quad 0 \quad 880.37)^{\mathrm{T}}, \ \mathbf{f}(0,2) = (55.229 \quad 0 \quad 398.34)^{\mathrm{T}}. \tag{63}$$

The remaining values are mirror symmetric to have the opposite signs at the moments, for instance, $\mathbf{f}(4,0) = (\,75.895 \quad 0 \quad 207.26\,)^{\mathrm{T}}$, etc. The solution can be now written according to (49)

$$\mathbf{d}(n,m) = \sum_{n'=0}^{6}\sum_{m'=0}^{4}\mathbf{G}_{7,5}(n-n', m-m')\mathbf{f}(n',m') + \mathbf{YC}, \tag{64}$$

where the Green's function is given by expression (47).

Example 4.5. For more complicated structural patterns, we can often write $\mathbf{d}(n,0) = \mathbf{d}(n,M)$ and/or $\mathbf{d}(0,m) = \mathbf{d}(N,m)$ despite the displacements at the opposite edges of a plate being not equal, and a virtual interlayer needs to be introduced. Consider the triangular honeycomb panel depicted in Fig. 5(a), where a pair of adjacent nodes represents the repeating nodal location, Fig. 5(b), and the lattice shown in Fig. 5(c) gives the associate substructure. Then the virtual interlayer and numbering of repeating nodal sets can be introduced as shown in Fig. 5(d), so that the lower nodes of sets $(0,m)$ belong to the right edge of panel, and the upper ones to the left edge. This allows one to write formally $\mathbf{d}(0,m) = \mathbf{d}(6,m)$ and introduce only three $(N, M+1)$-periodic $(N = M = 6)$ boundary load functions, $\mathbf{f}(n,0)$, $\mathbf{f}(n,6)$ and $\mathbf{f}(0,m)$. For the bending

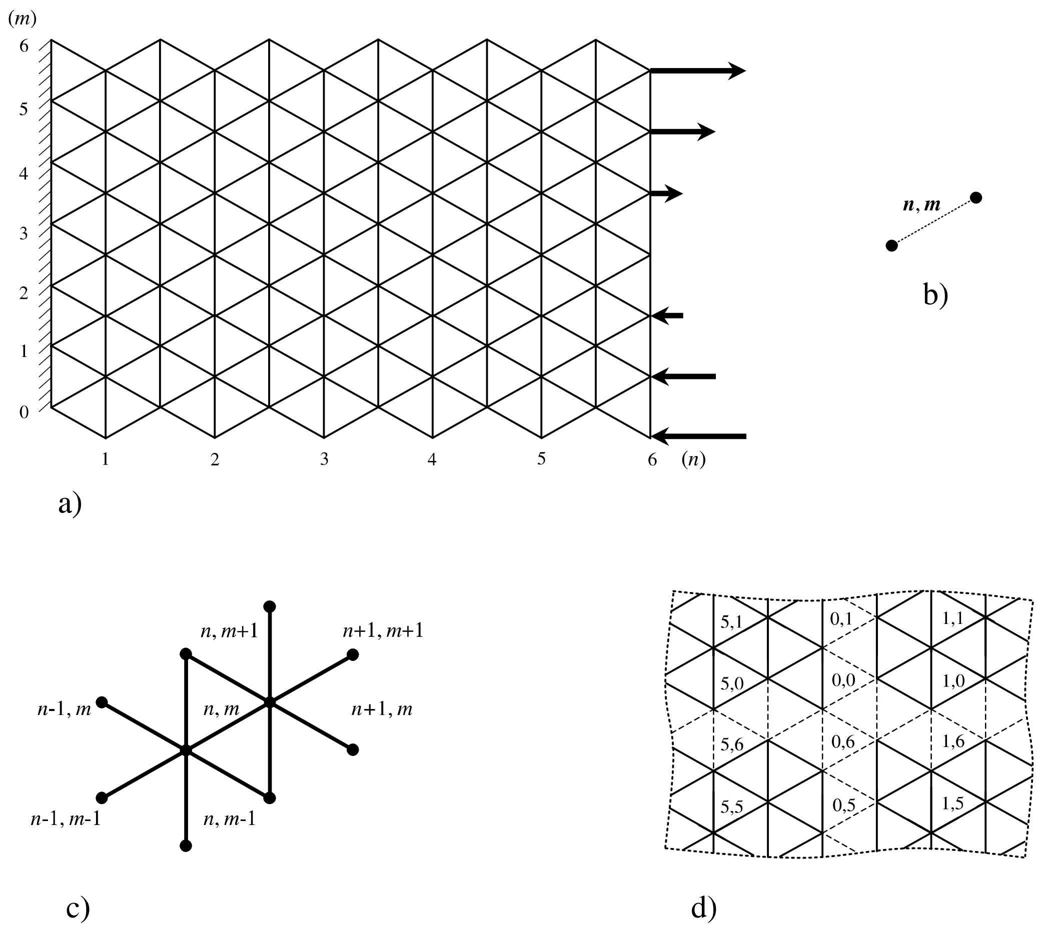

Fig. 5. Bending of a triangular honeycomb panel (a). Typical nodal location (b), associate substructure (c), virtual interlayer and numbering of nodal locations in the modified lattice (d).

problem shown in Fig. 5(a), the boundary conditions are mixed (either displacements or actual forces are specified at various locations). Thus the actual $\mathbf{f}^{(a)}$ and virtual $\mathbf{f}^{(v)}$ parts of the boundary loads have to be treated separately, as in Example 4.3, and the boundary conditions can be written as

$$\mathbf{f}^{(a)}(n,0)=\mathbf{f}^{(a)}(n,6)=\mathbf{0},\quad \mathbf{f}^{(a)}(0,m)=\begin{pmatrix} f_x^{(a)}(0,m) & f_y^{(a)}(0,m) & (m-3)P & 0\end{pmatrix}^{\mathrm{T}},$$
$$\mathbf{d}(0,m)=(\,0\quad 0\quad d_x(0,m)\quad d_y(0,m)\,)^{\mathrm{T}};\qquad n=0,1,\ldots,5,\quad m=0,1,\ldots,6; \tag{65}$$

where P describes the strength of the bending load, $f_{x,y}^{(a)}(0,m)$ are unknown support reactions at the left edge of the honeycomb, and $d_{x,y}(0,m)$ are unknown displacements at the right edge. Similar to the 1-D case (58), the stiffness matrix relationship for the virtual interlayer gives the compensation demand on the value of virtual terms $\mathbf{f}^{(v)}$. If considered together with the boundary (65) and equilibrium (50) conditions, it provides a sufficient system of linear equations for finding the unknown actual and virtual components of boundary loads, and vector $\mathbf{C}$. The sought solution then can be constructed as

$$\mathbf{d}(n,m)=\sum_{n'=1}^{5}(\mathbf{G}_{6,7}(n-n',m)\mathbf{f}(n',0)+\mathbf{G}(n-n',m-6)\mathbf{f}(n',6))+\sum_{m'=0}^{6}\mathbf{G}_{6,7}(n,m-m')\mathbf{f}(0,m')+\mathbf{YC}, \tag{66}$$

where the Green's function is found conventionally by using expression (47). If this structure is treated as pin-jointed, the non-trivial values of its kernel function read

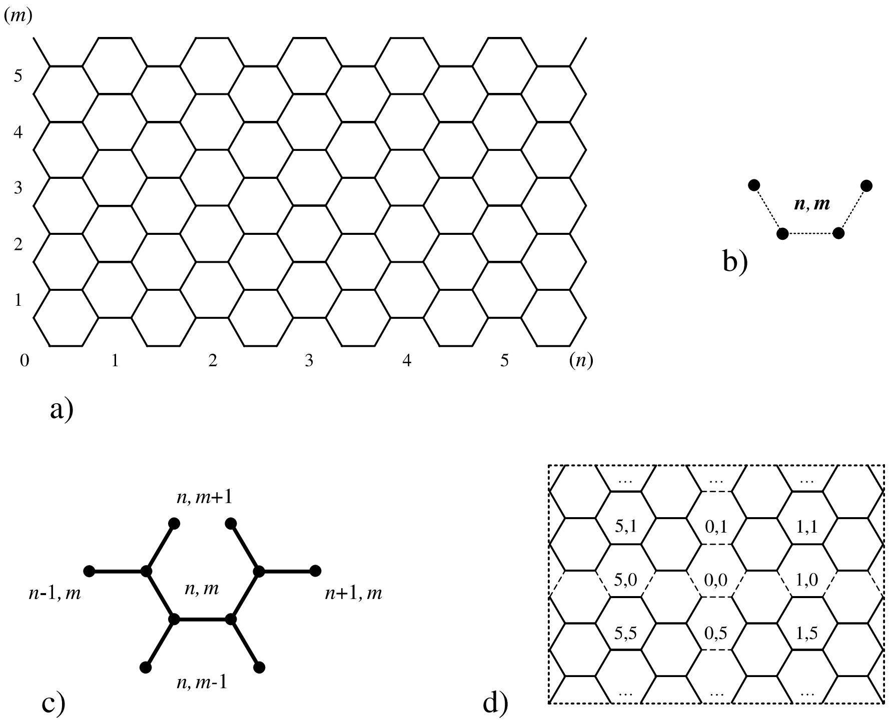

Fig. 6. Hexagonal honeycomb panel (a); typical nodal location (b), associate substructure (c), modified lattice (d).

$$\mathbf{K}(0,1)=\frac{EA}{4L}\begin{pmatrix}0&0&0&0\\0&-4&0&0\\-3&\sqrt{3}&0&0\\\sqrt{3}&-1&0&-4\end{pmatrix},\quad \mathbf{K}(1,0)=\frac{EA}{4L}\begin{pmatrix}0&0&0&0\\0&0&0&0\\-3&\sqrt{3}&0&0\\\sqrt{3}&-1&0&0\end{pmatrix},$$

$$\mathbf{K}(1,1)=\frac{EA}{4L}\begin{pmatrix}0&0&0&0\\0&0&0&0\\-3&-\sqrt{3}&0&0\\-\sqrt{3}&-1&0&0\end{pmatrix},\quad \mathbf{K}(0,0)=\frac{EA}{4L}\begin{pmatrix}12&0&-3&-\sqrt{3}\\0&12&-\sqrt{3}&-1\\-3&-\sqrt{3}&12&0\\-\sqrt{3}&-1&0&12\end{pmatrix},$$

$$\mathbf{K}(0,-1)=\mathbf{K}^{\mathrm{T}}(0,1),\quad \mathbf{K}(-1,0)=\mathbf{K}^{\mathrm{T}}(1,0)\quad\text{and}\quad \mathbf{K}(-1,-1)=\mathbf{K}^{\mathrm{T}}(1,1). \tag{67}$$

Example 4.6. Finally note that for the hexagonal honeycomb (Fig. 6(a)) under general boundary condition, only two pairs of (N,M)-periodic ($N=M=6$) functions, $\mathbf{f}(n,0)$, $\mathbf{f}(0,m)$ and $\mathbf{d}(n,0)$, $\mathbf{d}(0,m)$, are required to specify the boundary loads and displacements. Indeed, this holds if the typical nodal set, virtual interlayer and nodes' numbering are chosen as depicted in Fig. 6(b)–(d).

5. Conclusions

The static equilibrium state of finite repetitive lattices has been represented by a functional governing equation written in terms of the physical stiffness operator with a matrix function kernel. The operator acts as a discrete convolution sum over the kernel and displacement functions, and is written independent of boundary conditions to represent the structural properties only. The boundary conditions are taken into account at a subsequent stage of the analysis through a virtual load and substructure technique to formally close the structure and emulate cyclic symmetry. DFT has been utilised to solve the boundary value problem with the governing equations for both 1-D and 2-D lattices. The displacement solutions are sought as vector functions of discrete spatial parameters, to represent response of the lattice to static external loads and boundary conditions. These solutions have been written as discrete convolution sums over the Green's and external load functions. The Green's function does not depend on the beam or plate boundary conditions either, since it is obtained for the modified closed structure, and describes the basic response behaviour of the latter. The virtual boundary loads are included into the final solutions to eliminate the effect of the virtual substructure. Then the equivalence of static responses of the modified and original lattices is achieved, if the modified structure solution satisfies the original boundary conditions.

Being exact in the analytical sense, the approach can give essential savings in computational efforts, as compared with a direct matrix method. The numerical accuracy of the results can be affected only by the precision of a chosen finite element model for the associate substructure.

The approach can be extended to the free vibrations and dynamic response of regular lattices, where the governing equation is to be modified with a convolution mass operator, and the *dynamic* Green's function and virtual loads are to be introduced. The use of fast Fourier transform and analysis of non-rectangular plate-like lattices may also be worthy of separate studies.

Acknowledgements

This research was supported by a grant from the School of Engineering Sciences at the University of Southampton.

References

Avent, R.R., Issa, R.R.A., Chow, M.L., 1991. Discrete field stability analysis of planar trusses. Journal of Structural Engineering, ASCE 117 (2), 423–439.

Bracewell, R.N., 1986. The Fourier Transform and Its Applications, 2nd ed. McGraw-Hill, New York.

Damper, R.I., 1995. Introduction to Discrete-Time Signals and Systems. Chapman-Hall, London.

Dean, D.L., 1976. Discrete Field Analysis of Structural Systems. Springer, New York.

Dean, D.L., Avent, R.R., 1975. State of the art of discrete field analysis of space structures. In: Proceedings of the Second Conference on Space Structures. University of Surrey, Guildford, pp. 7–16.

Dean, D.L., Jetter, F.R., 1972. Analysis for truss buckling. ASCE Journal of the Engineering Mechanics Division 98, 1893–1897.

Dudgeon, D.E., Mersereau, R.M., 1984. Multidimensional Digital Signal Processing. Prentice-Hall, Englewood Cliffs.

Ellington, J.P., McCallion, H., 1957. Moments and deflections of a simply supported beam grillage. Aeronautical Quarterly 8, 360–368.

Issa, R.R.A., Avent, R.R., 1991. Microcomputer analysis of guided towers as lattices. Journal of Structural Engineering, ASCE 117 (4), 1238–1256.

Keane, A.J., Price, W.G., 1989. On the vibrations of mono-coupled periodic and near-periodic structures. Journal of Sound and Vibrations 128 (3), 423–450.

Kelley, W.G., Peterson, A.C., 2000. Difference Equations. Harcourt Academic Press, San Diego.

Langley, R.S., 1997. The response of two-dimensional periodic structures to impulsive point loading. Journal of Sound and Vibration 201 (2), 235–253.

Li, D., Benaroya, H., 1992. Dynamics of periodic and near-periodic structures. Applied Mechanics Reviews 45 (11), 447–460.

Mead, D.J., 1996. Wave propagation in continuous periodic structures: research contribution from Southampton. Journal of Sound and Vibration 190 (3), 495–524.

Moses, E., Ryvkin, M., Fuchs, M.B., 2001. A FE methodology for the static analysis of infinite periodic structures under general loading. Computational Mechanics 27, 369–377.

Noor, A.K., 1988. Continuum modelling for repetitive lattice structures. Applied Mechanics Reviews 41 (7), 285–296.

Renton, J.D., 1973. Buckling of long, regular trusses. International Journal of Solids and Structures 9 (12), 1489–1500.

Nuller, B.M., 1981. On elastic deformation of a layered plate and half space. In: Proceedings of the State Hydraulic Institute, 151. Energia, Leningrad, pp. 25–30 (in Russian).

Ryvkin, M., Fuchs, M.B., Nuller, B., 1999. Optimal design of infinite repetitive structures. Structural Optimisation 18, 202–209.

Samartin, A., 1988. Analysis of spatially periodic structures. Application to shell and spatial structures. In: Symposium of I.A.S.S. "Innovative Applications of Shell and Spatial Structures", Bangalore, India, Proceedings, Vol. III. Oxford and IBH Publishing Co., New Delhi, India, pp. 205–221.

Strang, G., 1988. Linear Algebra and Its Applications, 3rd Ed. Sauders, Philadelphia, P.A.